JOURNAL OF VIROLOGY, June 1991, p. 3219–3226
0022-538X/91/063219-08$02.00/0

Vol. 65, No. 6

A Domain at the 3′ End of the Polymerase Gene Is Essential for Encapsidation of Coronavirus Defective Interfering RNAs

ROBBERT G. VAN DER MOST, PETER J. BREDENBEEK,† AND WILLY J. M. SPAAN*

Department of Virology, Institute of Medical Microbiology, Faculty of Medicine, Leiden University, P.O. Box 320, 2300 AH Leiden, The Netherlands

Received 19 December 1990/Accepted 16 March 1991

Two murine hepatitis virus strain A59 defective interfering (DI) RNAs were generated by undiluted virus passages. The DI RNAs were encapsidated efficiently. The smallest DI particle, DI-a, contained a 5.5-kb RNA consisting of the following three noncontiguous regions from the MHV-A59 genome, which were joined in frame: the 5′-terminal 3.9 kb, a 798-nucleotide fragment from the 3′ end of the polymerase gene, and the 3′-terminal 805 nucleotides. A full-length cDNA clone of the DI-a genome was constructed and cloned downstream of the bacteriophage T7 promoter. Transcripts derived from this clone, pMIDI, were used for transfection of MHV-A59-infected cells and found to be amplified and packaged. Deletion analysis of pMIDI allowed us to identify a 650-nucleotide region derived from the 3′ end of the second open reading frame of the polymerase gene that was required for efficient encapsidation.

Coronaviruses are enveloped viruses containing a single-stranded infectious RNA genome. One of the best-studied members of this virus family is the murine coronavirus mouse hepatitis virus (MHV). During replication of MHV strain A59, six subgenomic mRNAs (sgRNAs) and genomic RNA which form a 3′-coterminal nested set are synthesized (for a review, see reference 28). In addition, all sgRNAs share a leader sequence with the 5′ end of the genome (13, 29).

The recent identification of subgenomic negative-stranded RNAs in coronavirus-infected cells (12, 26, 27) suggests that coronavirus sgRNAs function as RNA replicons. This would imply that antileader sequences present on the subgenomic negative strands contain replication signals for positive-strand synthesis.

These developments stress the need to develop a tool for studying *cis*-acting, regulatory sequences on the MHV genome. Since coronavirus genome-length clones are not available because of the very large size of the genome (approximately 30 kb [24]), an attractive strategy for studying these signals would involve the use of genomes of defective interfering (DI) particles. DI particles have truncated genomes which have retained replication signals but depend on proteins encoded by the standard virus for replication. The competition for the viral polymerase results in an interference with the replication of the standard virus. For Sindbis virus, sequences important for replication, encapsidation, and subgenomic RNA synthesis have successfully been identified by using a cDNA clone of a DI genome (8, 14, 15, 34). We wanted to determine whether this approach would be feasible for the characterization of coronavirus *cis*-acting signals.

One such signal is the packaging signal. Since MHV sgRNAs are not packaged, though trace amounts are sometimes detected in the purified virus (18), the encapsidation signal must be localized somewhere in the 20-kb region that is unique to the genome and not present in the sgRNAs. Since some DI RNAs are packaged, the encapsidation signal must be retained in the sequences of DI RNAs. One coronavirus DI genome that has been studied in more detail, DIssE (a 2.2-kb DI RNA obtained from MHV strain JHM [17, 20]), is not packaged efficiently and apparently lacks a specific RNA encapsidation signal (18).

In this article, we report the isolation of naturally occurring MHV-A59 DI RNAs which are efficiently packaged. We characterized the smallest of the DI RNAs, the 5.5-kb DI-a, and constructed a full-length DI cDNA clone. Transcripts derived from this construct, pMIDI, are amplified and packaged in the presence of standard virus. Deletion mutagenesis of pMIDI showed that a 650-nucleotide (nt) fragment located at the 3′ end of the second open reading frame (ORF) (ORF1b) of the polymerase gene (4) was necessary for packaging of DI RNA.

MATERIALS AND METHODS

Cells and viruses. Mouse DBT cells (11) and L cells (30) were grown in Dulbecco's modified Eagle's medium supplemented with 10% fetal calf serum. MHV-A59 was grown as described previously (30). A concentrated virus stock was prepared by polyethylene glycol 6000 precipitation, as described previously (30). DBT cells were used for propagation of virus; L cells were used for transfection experiments. Serial undiluted passages of MHV-A59 on DBT cells were performed as described by Makino et al. (20).

Isolation and analysis of viral RNAs. Viral RNAs were isolated from infected DBT or L cells as described previously (30). Poly(A)-containing RNA was obtained by using oligo(dT)-cellulose column chromatography (22). To obtain viral genomic RNA, virus-containing medium was harvested 20 h postinfection (p.i.) from an MHV-infected roller bottle culture of DBT or L cells and precipitated with polyethylene glycol 6000. Purification of virus on sucrose gradients and isolation of viral genomic RNA were carried out as described

* Corresponding author.
† Present address: Department of Molecular Microbiology, Washington University School of Medicine, Box 8093, 660 S. Euclid Ave., St. Louis, MO 63110-1093.

previously (30). RNA was denatured by incubation at 65°C for 5 min in a buffer containing 10 mM phosphate (pH 6.8), 50% formamide, 2.2 M formaldehyde, and 0.5 mM EDTA. Denatured RNA samples were analyzed on 1% agarose–1.1 M formaldehyde gels in 10 mM phosphate buffer (pH 6.8). For hybridization with nick-translated probes (22), RNA was transferred to GeneScreen Plus membranes (Dupont, NEN Research Products). RNA electrophoresis, transfer, and hybridization were performed as described previously (6). Hybridization with 5′-end-labelled oligonucleotides (23) in dried gels was carried out as described previously (7, 16). Three synthetic oligonucleotides were used for hybridization experiments: an oligonucleotide complementary to the 3′ end of the MHV genome (5′ GATTCTTCCAATTGGCC 3′) (1), an oligonucleotide complementary to nt 26 to 45 of the MHV-A59 leader sequence (5′ GTTTTAGAGTTGAGAG GGTA 3′) (24), and an oligonucleotide complementary to nt 153 to 170 of the 5′ end of the MHV-A59 genome (5′ CGTCACTGGCAGAGAACG 3′) (24).

cDNA synthesis and cloning. cDNA was synthesized according to the method of Gubler and Hoffmann (9) by using poly(A)-selected RNA as a template and oligo(dT) as a primer. Avian myeloblastosis virus reverse transcriptase was obtained from Pharmacia. Homopolymeric tailing and cloning of double-stranded cDNA were performed as described previously (4). For transformations (10), *Escherichia coli* PC2495 was used.

Construction of plasmids. pPARA. Genomic cDNA clones P005 (24) and pRG68 (2) were used to reconstruct the 5′- and 3′-terminal sequences, respectively, of the genome. To clone the 5′ end of the genome downstream of the bacteriophage T7 promoter, a 0.9-kb *Rsa*I fragment from clone P005 was ligated to a double-stranded synthetic linker

```
5′ TCGACGAAATTAATACGACTCACTATAGGGTATAAGAGTGATTGGCGTCCGTACGT 3′
3′     GCTTTAATTATGCTGAGTGATATCCCATATTCTCACTAACCGCAGGCATGCA 5′
```

containing a *Sal*I adaptor, the T7 promoter, and the 5′-terminal sequence of MHV-A59 upstream of the *Rsa*I site. This *Sal*I-*Rsa*I fragment was cloned into *Sal*I-cut pUC9. The resulting plasmid was digested with *Bam*HI and religated. Following bacterial transformation and plasmid isolation, the construct was digested with *Bam*HI and *Eco*RI, and a 0.85-kb *Bam*HI-*Eco*RI fragment from clone P005 was inserted, yielding a construct in which the first 1.3 kb of the MHV-A59 sequence was cloned downstream of the T7 promoter. To reconstruct the 3′ end of the genome, the 635-bp *Eco*RI-*Bcl*I fragment from clone pRG68 was ligated to a synthetic linker

```
5′ GATCATGGCCAATTGGAAGAATCACAAAA     3′
3′     TACCGGTTAACCTTCTTAGTGTTTTTCGA 5′
```

that contains the MHV-A59 3′-terminal sequence downstream of the *Bcl*I site, followed by a *Hin*dIII adaptor. The vector pUC18 was digested with *Eco*RI and made blunt with the Klenow fragment of DNA polymerase I (Boehringer). After insertion of a *Sal*I linker and digestion with *Sal*I and *Hin*dIII, the *Sal*I-*Eco*RI fragment containing the 5′ end of the genome and the *Eco*RI-*Hin*dIII fragment containing the 3′ end of the genome were ligated into this vector. The *Hin*dIII site of this construct pPA was converted into a *Nhe*I site by filling in with the Klenow fragment of DNA polymerase I, yielding plasmid pPAR. Plasmid pPAR does not contain a poly(A) tail at the 3′ end; to add a poly(A) tail to pPAR, the *Bam*HI-*Hin*dIII insert of pPA was isolated and treated with nuclease S1 (22), and a poly(A) tail was added by homopolymeric tailing using dATP (22). Likewise, a poly(T) tail was added to a filled-in *Hin*dIII site of pUC18. The A-tailed insert was annealed to the T-tailed vector, and the resulting construct was digested with *Eco*RI and religated to generate pPAH, which contained the 3′-terminal *Eco*RI-*Hin*dIII fragment with a poly(A) tail. Sequence analysis showed that the poly(A) tail synthesized in this way contained approximately 50 A residues. The plasmid pPAN was obtained by converting the *Hin*dIII site of pPAH to a *Nhe*I site. To clone the poly(A) tail into pPAR, a unique *Sac*I site located 52 nt upstream the *Bcl*I site was used. Thus, the smaller *Sac*I-*Nhe*I fragment from pPAN, containing the poly(A) tail, was cloned into *Sac*I-*Nhe*I-cut pPAR, yielding pPARA.

pMIDI. A 3.4-kb *Eco*RI fragment from DI cDNA clone pDI01 was inserted into the unique *Eco*RI site of pPARA, yielding plasmid pMIDI.

pMIDIΔH. pMIDI was digested with *Hin*dIII; the large *Hin*dIII fragment was isolated and religated, yielding pMIDIΔH.

pMIDIΔEH. An internal 1,363-nt *Pst*I fragment from pMIDI was deleted, yielding pMIDIΔP, from which the unique *Eco*RI site was removed by filling in the recessed 3′ ends with the Klenow fragment of DNA polymerase I. Subsequently, the 1,363-nt *Pst*I fragment was inserted back into the *Pst*I site. This plasmid was digested with *Eco*RI and *Hin*dIII, and the large *Eco*RI-*Hin*dIII fragment was religated after the recessed 3′ ends were filled in. Finally, the *Mlu*I-*Sac*I fragment from this construct, containing the filled-in *Eco*RI site, was deleted, and the corresponding *Mlu*I-*Sac*I fragment from pMIDI was inserted, yielding pMIDIΔEH.

pMIDIΔE. pPARA was digested with *Eco*RI and made blunt with the Klenow fragment of DNA polymerase I, and a *Bgl*II linker was inserted into the filled-in *Eco*RI site. After digestion with *Bgl*II and treatment with mung bean nuclease (22), the construct was ligated, yielding pMIDIΔE.

M13 cloning and DNA sequencing. Restriction fragments of DI cDNA clone pDI01 were subcloned in M13 vectors by standard procedures (22). Single-stranded DNA from M13 clones was sequenced with the Klenow fragment of DNA polymerase I (25) and [α-^{32}P]dATP or T7 DNA polymerase (33) (Pharmacia) and [α-^{35}S]dATP, according to the instructions of the manufacturer. Sequence data were analyzed by using the computer programs of Staden (31).

In vitro transcription and transfection. Plasmid DNAs were linearized with *Nhe*I. In vitro transcription was done as described previously (3). Transfection of L cells with lipofectin (Bethesda Research Laboratories) was performed as described by Grakoui et al. (8), with some minor modifications. Monolayers of L cells in 35-mm dishes were first infected with MHV-A59 at a multiplicity of infection of 10. After 1 h, the inoculum was removed and a mixture, containing 1 μg of RNA and 10 μl of lipofectin in 200 μl of phosphate-buffered saline, that had been preincubated on ice for 10 min was added. After a 10-min incubation at room temperature, the transfection mixture was removed, and cells were washed and further incubated at 37°C in the presence of OptiMEM (GIBCO).

Nucleotide sequence accession number. The nucleotide sequence data reported in this article have been assigned the EMBL nucleotide sequence data base accession number X57302.

RESULTS

DI RNAs are generated during undiluted virus passage. To obtain MHV-A59 DI particles, 20 serial undiluted passages on murine DBT cells were carried out. During the later

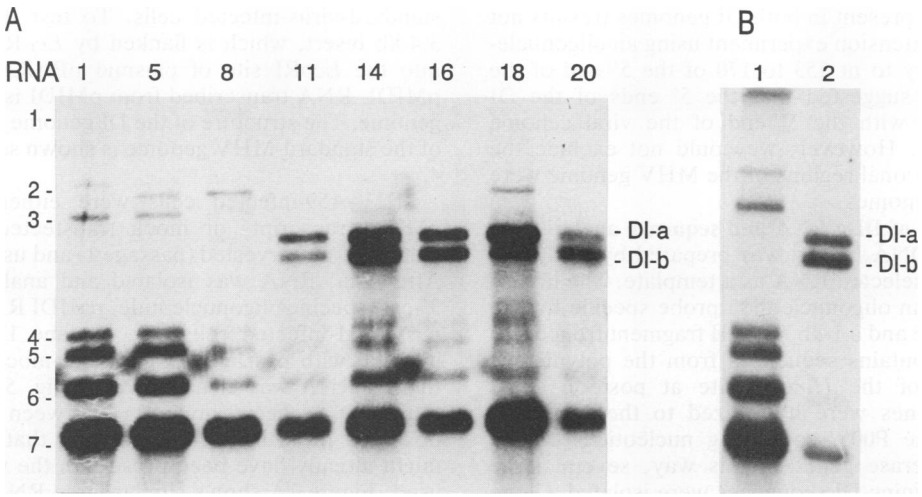

FIG. 1. Hybridization analysis of intracellular RNA. The 3'-end-specific oligonucleotide was used as a probe. (A) Analysis of RNA from undiluted passages. The number above each lane indicates the passage of the virus used to infect DBT cells from which RNA was isolated. The MHV-A59 sgRNAs are numbered according to the method of Cavanagh et al. (5). DI RNAs are indicated. (B) Intracellular RNA after two serial high-dilution passages (lane 1) and intracellular RNA after two undiluted passages (lane 2).

passages, the formation of syncytia was delayed and less severe compared with their formation during the early passages. Medium (200 μl) from a number of these passages was used to infect fresh monolayers of DBT cells, from which RNA was isolated at 8 h p.i. Analysis of intracellular RNA showed the appearance of several new RNA species during serial undiluted passages (Fig. 1A). At passage 5, a large RNA species migrating between RNAs 2 and 3 was observed, which disappeared between passages 8 and 11 and reappeared at passage 18. Furthermore, after 8 to 11 undiluted passages, two RNA species of 5.5 and 6.5 kb were detected and remained present during further passage. Additionally, a very large RNA species of about genome size was observed in passages 8 and 18. Fifty-percent tissue culture infective dose analysis showed a 1.8-log-unit fluctuation in virus titers (results not shown).

To determine whether the replication of the 5.5- and 6.5-kb RNA species depended on standard-virus functions, two high-dilution passages of a passage 18 virus stock were performed. DBT cells were infected at a multiplicity of infection of 0.0002. A second passage was carried out at a multiplicity of infection of 0.1. Medium from this second passage was used to infect DBT cells from which RNA was isolated at 8 h p.i. Analysis of the RNA showed that both the 5.5- and 6.5-kb RNA species disappeared after two high-dilution passages (Fig. 1B, lane 1). In contrast, a control experiment showed that the RNA species were still present after two undiluted passages with passage 18 virus (Fig. 1B, lane 2). These results demonstrate that the replication of these RNAs is dependent on the presence of standard virus. It can also be seen in Fig. 1B that the synthesis of all MHV-A59-specific mRNAs is severely inhibited in the presence of the 5.5- and 6.5-kb RNA species. These data strongly suggested that both RNAs are DI RNAs. They were therefore termed DI-a and DI-b as indicated in Fig. 1A.

Characterization of DI RNAs. Encapsidation of MHV-A59 DI RNAs was studied by hybridization analysis of RNA isolated from purified virus. Virus was isolated from medium of cells infected with a DI-containing virus stock. Analysis of virion RNA showed that the DI-a and DI-b RNAs are efficiently packaged (Fig. 2, lane 3), suggesting that these DI RNAs contain a specific RNA packaging signal. Figure 2 also shows clearly that no sgRNAs of MHV were packaged.

From hybridization analysis using various oligonucleotides and restriction fragments as probes, it could be deduced that 5'-terminal and 3'-terminal sequences of the

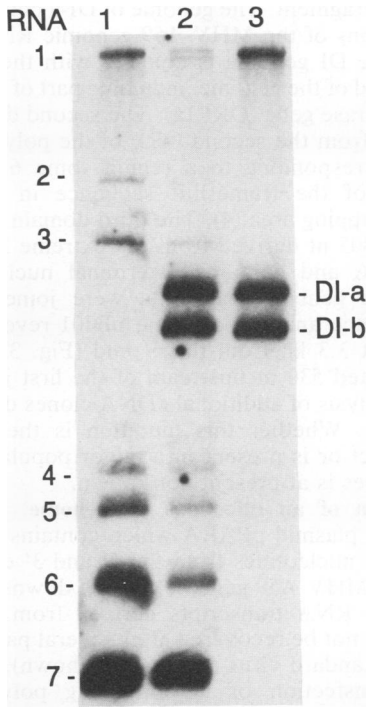

FIG. 2. Hybridization analysis of intracellular and viral genomic RNA. The 3'-end-specific oligonucleotide was used as a probe. Intracellular RNA from cells infected with wild-type MHV-A59 (lane 1) or MHV-A59 with DI particles (lane 2) and viral genomic RNA from a DI-containing MHV-A59 stock (lane 3) were analyzed. DI-a and DI-b RNAs are indicated.

MHV genome were present in both DI genomes (results not shown). A primer extension experiment using an oligonucleotide complementary to nt 153 to 170 of the 5′ end of the MHV-A59 genome suggested that the 5′ ends of the DI RNAs are colinear with the 5′ end of the viral genome (results not shown). However, we could not exclude the possibility that additional regions of the MHV genome were present in the DI genomes.

Molecular cloning of DI-a RNA and sequence analysis. An oligo(dT)-primed cDNA library was prepared by using DI-containing poly(A)-selected RNA as a template. The library was screened with an oligonucleotide probe specific for the 3′ end of the genome and a 1-kb *Hin*dIII fragment from clone P005 (24), which contains sequences from the polymerase gene downstream of the *Hin*dIII site at position 1984. Double-positive clones were hybridized to the *Nar*I-*Pst*I fragment from clone P005, containing nucleotides 180 to 1140 of the polymerase gene. In this way, several large cDNA clones containing DI sequences were isolated. Clone pDI01 with a 5.2-kb insert was used for further analysis. Restriction enzyme and Southern blot analysis of this cDNA clone enabled us to determine a restriction map of the DI genome, which is shown in Fig. 3A. From this restriction map, we could conclude that the 5′ end of the insert in pDI01 is colinear with the 5′ end of the MHV genome, indicating that pDI01 contains a cDNA of the 5.5-kb DI-a.

These data, in combination with the results obtained by primer extension and hybridization analysis of DI-a, suggested that the 5′ and 3′ ends of he DI genome are similar to the corresponding regions of the genomic RNA. We therefore chose to sequence only the 3.4-kb *Eco*RI fragment from pDI01 in which the junctions between various genomic fragments should be located. Figure 3B shows the sequence of the *Eco*RI fragment. The genome of DI-a consists of three different regions of the MHV-A59 genomic RNA. The first domain of the DI genome is colinear with the first 3.9 kb from the 5′ end of the genome, including part of the first ORF of the polymerase gene (ORF1a). The second domain of 798 nt is derived from the second ORF of the polymerase gene (ORF1b), corresponding to a region some 6.3 to 7.1 kb downstream of the frameshift sequence in the ORF1a-ORF1b overlapping area (4). The third domain consists of a sequence of 805 nt derived from the extreme 3′ end of the genomic RNA and contains C-terminal nucleocapsid sequences. The genome fragments were joined in frame, though sequence analysis of clone pDI01 revealed a UAA stop codon at 3.3 kb from the 5′ end (Fig. 3B); this stop codon is located 530 nt upstream of the first junction site. Sequence analysis of additional cDNA clones did not reveal this mutation. Whether this mutation is the result of a cloning artifact or is present in a minor population of DI-a RNA molecules is at present not known.

Construction of an infectious DI genome. Initially, we constructed a plasmid pPARA which contains the terminal 1,319 and 680 nucleotides from the 5′ and 3′ ends, respectively, of the MHV-A59 genome, cloned downstream of the T7 promoter. RNA transcripts derived from the plasmid pPARA could not be recovered after several passages in the presence of standard virus (results not shown). In contrast, following transfection of DI-containing poly(A)-selected RNA in the presence of standard virus, DI-a RNA, which contains a 3.4-kb insert extra compared with pPARA transcripts, is amplified and packaged into DI particles (results not shown). This strongly suggests that the 3.4-kb insert contains a replication or encapsidation signal that is essential for recovery of DI particles from DI RNA-transfected and standard-virus-infected cells. To test this hypothesis, the 3.4-kb insert, which is flanked by *Eco*RI sites, was cloned into the *Eco*RI site of plasmid pPARA, yielding plasmid pMIDI. RNA transcribed from pMIDI is similar to the DI-a genome. The structure of the DI genome compared with that of the standard-MHV genome is shown schematically in Fig. 4.

MHV-A59-infected cells were either transfected with pMIDI transcripts or mock transfected. Ten hours p.i., medium was harvested (passage 1) and used to infect L cells. After 7 h, RNA was isolated and analyzed by using the 3′-end-specific oligonucleotide. pMIDI RNA was detected in passage 1-infected cells (Fig. 5, lane 1), whereas in cells infected with passage 1 virus from mock-transfected cells, this DI RNA was clearly absent (Fig. 5, lane 2). An additional RNA species migrating between RNAs 2 and 3 is observed in both lanes, suggesting that this RNA species might already have been present in the virus stock that we used. Figure 1A shows similar large RNA species.

These data demonstrate that a synthetic DI RNA, constructed from genomic and DI-specific sequences, is amplified and passaged efficiently in the presence of standard virus.

Identification of the packaging signal. To obtain more insight into the nature and location of the signal present in the 3.4-kb insert, we constructed several deletion mutants of pMIDI (Fig. 6A). Because the genome fragments were joined in frame in pMIDI, we constructed these mutants such that they, too, had in-frame fusions. Transcripts from these mutants were used to transfect standard-virus-infected L cells. Intracellular RNA was analyzed by hybridization with 5′-end-specific probes (see legend to Fig. 6). The 5′-end-specific probes were used to avoid detection of sgRNAs since the DI RNAs could comigrate with the MHV-A59 sgRNAs, which would obscure detection of the DI RNAs.

Figure 6B shows that RNA of the three deletion constructs was detected in transfected cells (Fig. 6B, lanes 1 through 4). The amount of pMIDIΔE RNA was much larger at 12 h p.i. than at 9 h p.i., indicating that amplified RNA rather than input RNA was detected (Fig. 6B, compare lanes 1 and 2). A similar result was obtained for pMIDIΔH RNA.

To determine whether the RNAs are packaged, progeny virus from transfected cells was harvested at 12 h p.i. and passaged once. This virus was then used to infect L cells, and intracellular RNA was analyzed. pMIDIΔH RNA and pMIDIΔEH RNA were readily detected, but pMIDIΔE RNA was not present (Fig. 6B, lanes 6 through 8), indicating that both pMIDIΔH RNA and pMIDIΔEH RNA are packaged. To confirm the encapsidation of both pMIDIΔH and pMIDIΔEH RNA, we purified virus from second-passage medium and isolated viral RNA. Hybridization analysis demonstrated clearly that both DI RNAs are efficiently packaged (Fig. 7). Thus, sequences required for encapsidation have not been removed from these RNAs. However, since pMIDIΔE cannot be passaged, this RNA apparently lacks these sequences. These results strongly suggest that the packaging signal is located on an 800-nt *Hin*dIII-*Eco*RI fragment containing 650 nt derived from the 3′ end of ORF1b and 150 nt from the nucleocapsid gene, which is removed from the pMIDIΔE sequence and which is still present in the pMIDIΔEH sequence (Fig. 6A). Since MHV sgRNAs are not packaged, the 650-nt fragment that is derived from the 3′ end of ORF1b must contain the packaging signal.

In progeny virus from mock-transfected cells and from cells transfected with pMIDIΔE RNA, a larger RNA species (Fig. 6B, lanes 6 and 9) which had already been detected in

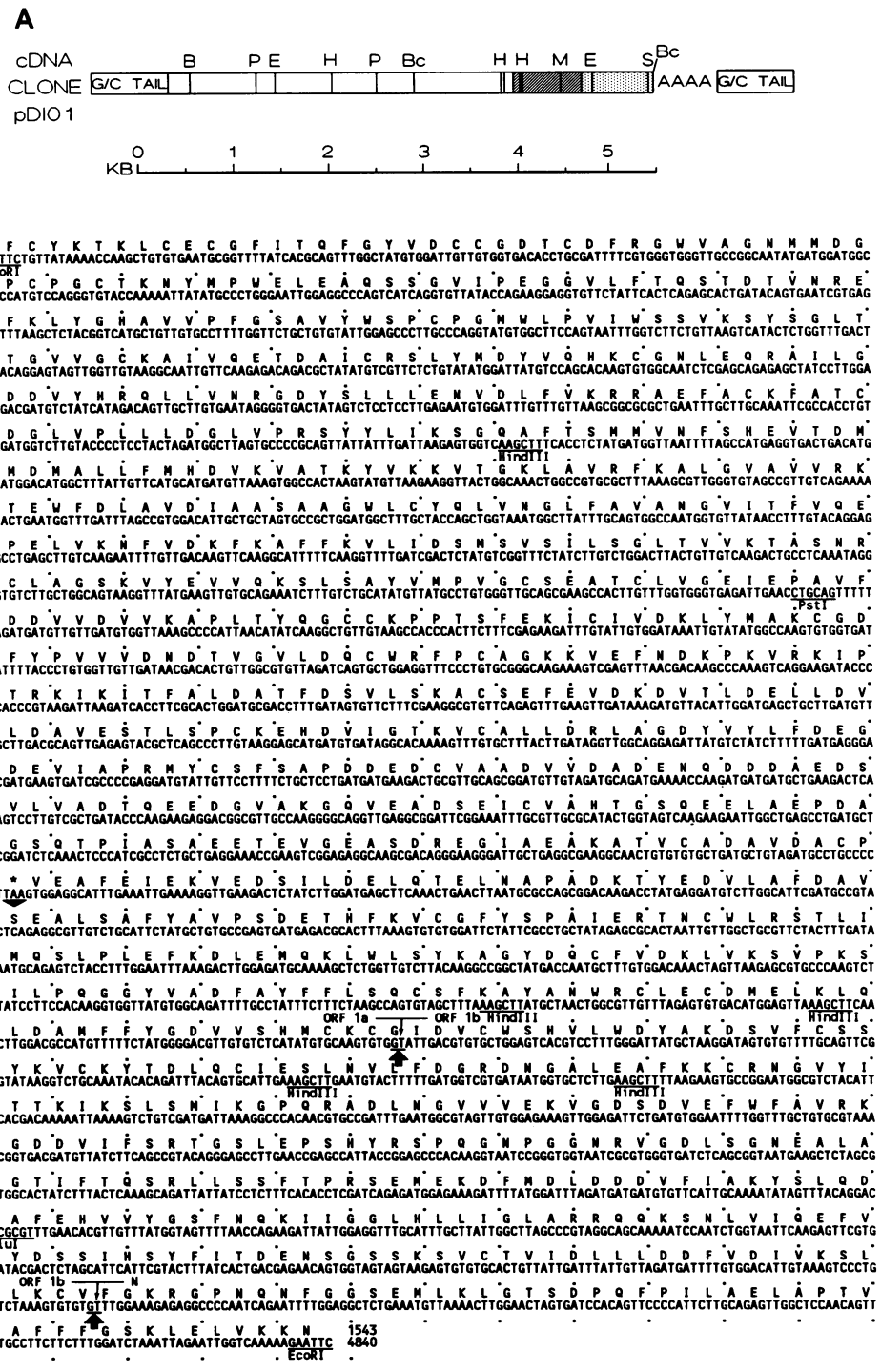

FIG. 3. Structure of DI-a. (A) Restriction map of cDNA clone pDI01. B, *Bam*HI; Bc, *Bcl*I; E, *Eco*RI; H, *Hin*dIII; M, *Mlu*I; P, *Pst*I; S, *Sac*I. The open bars represent sequences derived from ORF1a, the cross-hatched bar indicates sequences derived from ORF1b, and the dotted bars represent sequences derived from the 3′ end. (B) Nucleotide sequence of the *Eco*RI fragment of cDNA clone pDI01 and the predicted amino acid sequence of the major ORFs. Nucleotides are numbered starting at the 5′ end of the MHV-A59 genome (24). The UAA stop codon is indicated by an asterisk and an arrowhead. Several restriction sites are underlined. Arrows indicate the sites at which the sequence fusions occurred.

other experiments (Fig. 3A, lane 2 and Fig. 5) was observed. The results shown in Fig. 6B indicate that this RNA species is amplified to a detectable level only in the absence of a more efficiently replicating DI RNA.

DISCUSSION

The data presented in this article show that new RNA species are rapidly generated during serial undiluted pas-

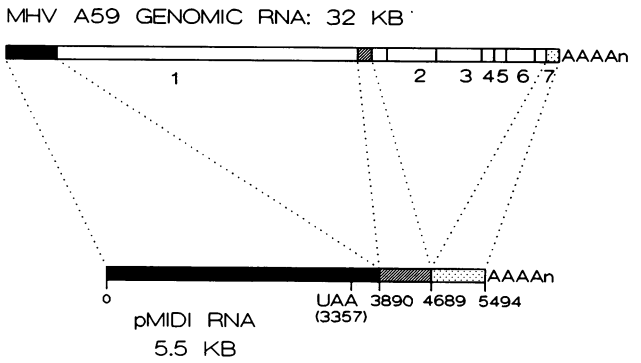

FIG. 4. A comparison of the structures of pMIDI RNA and the MHV-A59 genomic RNA. The UAA stop codon and positions of the fusion sites are indicated. Black bars indicate sequences derived from the 5′ end of the genome; other symbols are the same as for Fig. 3A.

sages of MHV-A59. A number of observations indicate that these new RNA species are DI RNAs. First, the RNAs interfere with the replication of the standard virus both at the level of mRNA synthesis and at the level of virus infectivity. Second, the RNA species are eliminated from the standard-virus stock after two high-dilution passages, demonstrating that replication of the RNAs depends on standard-virus functions. Because the DI RNAs are to be used as RNA vectors, we were interested in DI RNAs that were stable during virus passage; obviously, with the generation of DI-a and DI-b, we succeeded in obtaining such stable DI RNAs.

The MHV-A59 DI-a and DI-b RNAs are encapsidated efficiently. This indicates that both the DI RNAs contain a specific RNA packaging signal, in contrast to the inefficiently packaged DIssE RNA (18).

We constructed a cDNA clone, pMIDI, containing DI-a-specific as well as viral genomic sequences. The structure of

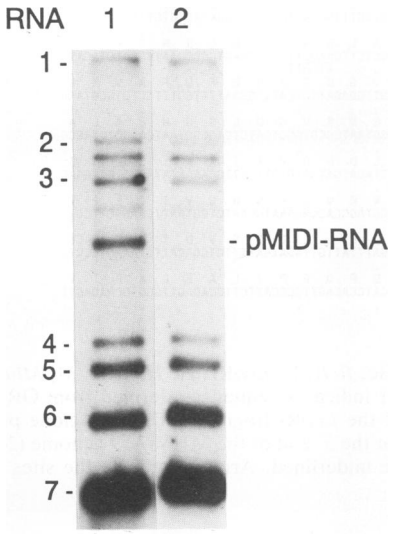

FIG. 5. Analysis of intracellular RNA after transfection or mock transfection. The 3′-end-specific oligonucleotide was used as a probe. L cells were either transfected with pMIDI transcripts (lane 1) or mock transfected (lane 2). First-passage medium was used to infect L cells. RNA was isolated at 7 h p.i.

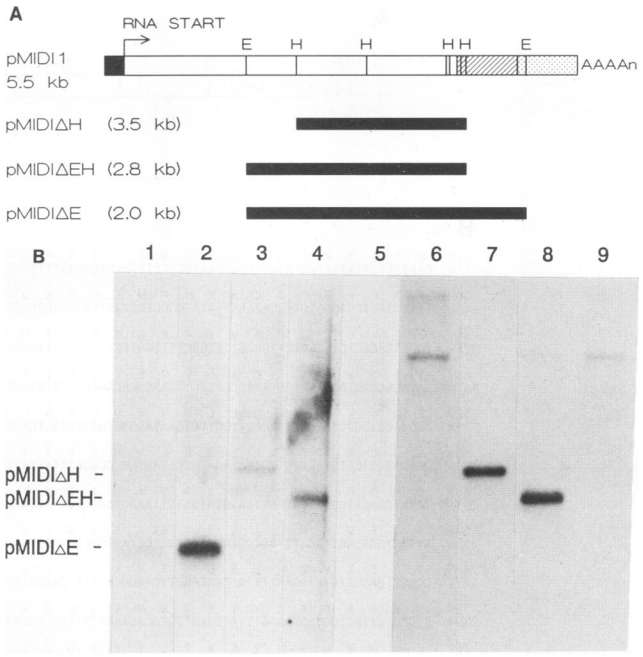

FIG. 6. (A) Schematic representation of the deletion mutants that were constructed from pMIDI. Deletions are indicated by black bars; lengths of the transcripts are indicated. Other symbols and abbreviations are the same as for Fig. 3A. (B) Hybridization analysis of intracellular RNA. L cells were either transfected with transcripts of pMIDI deletion mutants or mock transfected. RNA isolated from transfected cells was analyzed by hybridization with the *Nar*I-*Pst*I fragment from clone P005, containing nucleotides 180 to 1140 from the 5′ end of the MHV genome. RNA that was isolated from cells that were infected with second-passage virus was analyzed by hybridization with the 5′-end-specific oligonucleotide. Lane 1 shows RNA isolated from transfected cells at 9 h p.i., lanes 2 to 5 show RNA samples isolated from transfected cells at 12 h p.i., and lanes 6 to 9 show RNA samples isolated from cells infected with second-passage virus. Lanes: 1, 2, and 6, pMIDIΔE; 3 and 7, pMIDIΔH; 4 and 8, pMIDIΔEH; 5 and 9, mock transfections.

pMIDI RNA is similar to the structure of DI-a. Transfected RNA transcripts synthesized from pMIDI were amplified efficiently in the presence of standard virus and could be detected after several passages. From this, we conclude that the pMIDI sequence contains replication signals as well as the RNA packaging signal(s) which will allow the identification and analysis of *cis*-acting signals.

pMIDI was used to construct several deletion mutants. RNA from the mutants in which sequences derived from ORF1b were retained, pMIDIΔEH and pMIDIΔH, was readily detected in transfected cells, in infected cells after one passage, and in purified virus. In contrast, RNA from pMIDIΔE, lacking all sequences from ORF1b, was amplified in transfected cells but was not detected after passaging. This indicates that this construct lacks an encapsidation signal, implying that the replication and encapsidation signals do not overlap and can therefore be studied separately. The specificity of the packaging signal is demonstrated by the observation that pMIDIΔE RNA, though detected in transfected cells in much larger quantities than pMIDIΔEH and pMIDIΔH RNA, cannot be passaged. From a comparison of the pMIDIΔE and pMIDIΔEH sequences and because the MHV sgRNAs are not packaged, we conclude that packaging of DI RNAs depends on sequences located in a

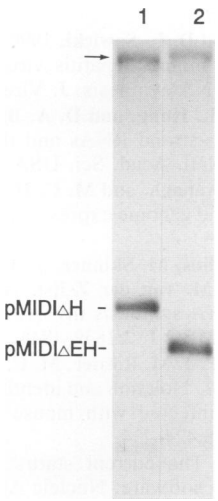

FIG. 7. Hybridization analysis of viral genomic RNA from purified virus. The 3′-end-specific oligonucleotide was used as a probe. Lane 1, pMIDIΔH; lane 2, pMIDIΔEH. DI RNAs are indicated, and viral genomic RNA is marked by an arrow.

fragment of 650 nt derived from the 3′ end of the second ORF of the 20-kb polymerase gene. Since pMIDIΔH RNA is almost identical in size to sgRNA4, which is not packaged, it is very unlikely that a size constraint is responsible for specific packaging.

Very recently, Makino et al. reported the sequence of an efficiently encapsidated MHV-JHM DI RNA, DIssF (21). By comparing the sequences from DIssE (19) and DIssF, the authors located the packaging signal on a fragment of 1,480 nt consisting of sequences derived from two domains of ORF1a and from one domain at the 3′ end of ORF1b (21). If we now compare this 1,480-nt fragment with the 650-nt fragment that we have identified, the packaging signal can be narrowed down to a stretch of 347 nt at the 3′ end of ORF1b corresponding to nt 4040 and 4387 of the pMIDI genome (Fig. 3B). This identification was confirmed by the recent observation that a 2.4-kb RNA containing 400 nt derived from ORF1b, corresponding to nt 4040 to 4440 (Fig. 3B), is packaged efficiently (unpublished results).

In contrast to the MHV sgRNAs, the bovine coronavirus sgRNAs are encapsidated (12). This could be due to an aspecific and inefficient mode of encapsidation or, alternatively, the bovine coronavirus encapsidation signal could be located within the leader sequence or within the 3′ end of the genome, which is present in each sgRNA.

The location of an RNA packaging signal within the sequence of ORF1b sheds an interesting light on the data obtained by Stohlman et al. (32) concerning the interaction between MHV leader RNA and the nucleocapsid protein. The authors suggest that either an additional signal or a size constraint determines MHV encapsidation. Since our results argue for the first option, it will be interesting to study the possible interaction between the nucleocapsid protein and the encapsidation signal. A specific interaction between an RNA packaging signal and the nucleocapsid protein for Sindbis virus has recently been described (34).

A more detailed deletion mutagenesis of the region containing the encapsidation signal will allow us to identify the precise nature and location of the encapsidation signal. Other experiments will also include the insertion of an intergenic region into the DI cDNA clones, which will enable us to study MHV subgenomic RNA synthesis.

ACKNOWLEDGMENTS

We thank Caroline Brown, Raoul de Groot, Willem Luytjes, and Eric Snijder for critical reading of the manuscript and for helpful discussions.

R.G.M. is supported by grant 331-020 from the Dutch Organization for Chemical Research (SON). P.J.B. was supported by the Institute of Molecular Biology.

REFERENCES

1. **Armstrong, J., S. Smeekens, and P. Rottier.** 1983. Sequence of the nucleocapsid gene from murine coronavirus MHV-A59. Nucleic Acids Res. **11**:883–891.
2. **Bredenbeek, P. J., J. Charite, J. F. Noten, W. Luytjes, M. C. Horzinek, B. A. M. van der Zeijst, and W. J. Spaan.** 1987. Sequences involved in the replication of coronaviruses. Adv. Exp. Med. Biol. **218**:65–72.
3. **Bredenbeek, P. J., A. F. H. Noten, M. C. Horzinek, and W. J. M. Spaan.** 1990. Identification and stability of a 30-kDa nonstructural protein encoded by mRNA 2 of mouse hepatitis virus in infected cells. Virology **175**:303–306.
4. **Bredenbeek, P. J., C. J. Pachuk, A. F. H. Noten, J. Charite, W. Luytjes, S. R. Weiss, and W. J. M. Spaan.** 1990. The primary structure and expression of the 2nd open reading frame of the polymerase gene of the coronavirus MHV-A59—a highly conserved polymerase is expressed by an efficient ribosomal frameshifting mechanism. Nucleic Acids Res. **18**:1825–1832.
5. **Cavanagh, D., D. A. Brian, L. Enjuanes, K. V. Holmes, M. M. C. Lai, H. Laude, S. G. Siddell, W. Spaan, F. Taguchi, and P. J. Talbot.** 1990. Recommendations of the Coronavirus Study Group for the nomenclature of the structural proteins, messenger RNAs, and genes of coronaviruses. Virology **176**: 306–307.
6. **De Groot, R. J., J. Maduro, J. A. Lenstra, M. C. Horzinek, B. A. M. van der Zeijst, and W. J. Spaan.** 1987. cDNA cloning and sequence analysis of the gene encoding the peplomer protein of feline infectious peritonitis virus. J. Gen. Virol. **68**:2639–2646.
7. **De Vries, A. A. F., E. D. Chirnside, P. J. Bredenbeek, L. A. Gravestein, M. C. Horzinek, and W. J. M. Spaan.** 1990. A common leader sequence is spliced to all subgenomic mRNAs of equine arteritis virus. Nucleic Acids Res. **18**:3241–3247.
8. **Grakoui, A., R. Levis, R. Raju, H. V. Huang, and C. M. Rice.** 1989. A *cis*-acting mutation in the Sindbis virus junction region which affects subgenomic RNA synthesis. J. Virol. **63**:5216–5227.
9. **Gubler, U., and B. J. Hoffmann.** 1983. A simple and very efficient method for generating cDNA libraries. Gene **25**:263–269.
10. **Hanahan, D.** 1983. Studies on transformation of *Escherichia coli* with plasmids. J. Mol. Biol. **166**:557–580.
11. **Hirano, N., K. Fujiwara, S. Hino, and M. Matumoto.** 1974. Replication and plaque formation of mouse hepatitis virus (MHV-2) in mouse cell line DBT culture. Arch. Gesamte Virusforsch. **44**:298–302.
12. **Hofmann, M. A., P. B. Sethna, and D. A. Brian.** 1990. Bovine coronavirus mRNA replication continues throughout persistent infection in cell culture. J. Virol. **64**:4108–4114.
13. **Lai, M. M., R. S. Baric, P. R. Brayton, and S. A. Stohlman.** 1984. Characterization of leader RNA sequences on the virion and mRNAs of mouse hepatitis virus, a cytoplasmic RNA virus. Proc. Natl. Acad. Sci. USA **81**:3626–3630.
14. **Levis, R., S. Schlesinger, and H. V. Huang.** 1990. Promoter for Sindbis virus RNA-dependent subgenomic RNA transcription. J. Virol. **64**:1726–1733.
15. **Levis, R., B. G. Weiss, M. Tsiang, H. Huang, and S. Schlesinger.** 1986. Deletion mapping of sindbis virus DI RNAs derived from cDNAs defines the sequences essential for replication and packaging. Cell **44**:137–145.
16. **Luytjes, W., L. S. Sturman, P. J. Bredenbeek, J. Charite,**

B. A. M. van der Zeijst, M. C. Horzinek, and W. J. Spaan. 1987. Primary structure of the glycoprotein E2 of coronavirus MHV-A59 and identification of the trypsin cleavage site. Virology **161**:479–487.

17. **Makino, S., N. Fujioka, and K. Fujiwara.** 1985. Structure of the intracellular defective viral RNAs of defective interfering particles of mouse hepatitis virus. J. Virol. **54**:329–336.
18. **Makino, S., C. Shieh, J. G. Keck, and M. M. C. Lai.** 1988. Defective-interfering particles of murine coronavirus: mechanism of synthesis of defective viral RNAs. Virology **163**:104–111.
19. **Makino, S., C. Shieh, L, H. Soe, S. C. Baker, and M. M. C. Lai.** 1988. Primary structure and translation of a defective interfering RNA of murine coronavirus. Virology **166**:1–11.
20. **Makino, S., F. Taguchi, and K. Fujiwara.** 1984. Defective interfering particles of mouse hepatitis virus. Virology **133**:9–17.
21. **Makino, S., K. Yokomori, and M. M. C. Lai.** 1990. Analysis of efficiently packaged defective interfering RNAs of murine coronavirus: localization of a possible RNA packaging signal. J. Virol. **64**:6045–6053.
22. **Maniatis, T., E. F. Fritsch, and J. Sambrook.** 1982. Molecular cloning: a laboratory manual. Cold Spring Harbor Laboratory, Cold Spring Harbor, N.Y.
23. **Meinkoth, J., and G. Wahl.** 1984. Hybridization of nucleic acids immobilized on solid supports. Anal. Biochem. **138**:267–284.
24. **Pachuk, C. J., P. J. Bredenbeek, P. W. Zoltick, W. J. M. Spaan, and S. R. Weiss.** 1989. Molecular cloning of the gene encoding the putative polymerase of mouse hepatitis coronavirus, strain A59. Virology **171**:141–148.
25. **Sanger, F., S. Nicklen, and A. R. Coulson.** 1977. DNA sequencing with chain-terminating inhibitors. Proc. Natl. Acad. Sci. USA **74**:5463–5467.
26. **Sawicki, S. G., and D. L. Sawicki.** 1990. Coronavirus transcription: subgenomic mouse hepatitis virus replicative intermediates function in RNA synthesis. J. Virol. **64**:1050–1056.
27. **Sethna, B. P., S.-L. Hung, and D. A. Brian.** 1989. Coronavirus subgenomic minus-strand RNAs and the potential for mRNA replicons. Proc. Natl. Acad. Sci. USA **86**:5626–5630.
28. **Spaan, W., D. Cavanagh, and M. C. Horzinek.** 1988. Coronaviruses: structure and genome expression. J. Gen. Virol. **69**:2939–2952.
29. **Spaan, W., H. Delius, M. Skinner, J. Armstrong, P. Rottier, S. Smeekens, B. A. M. van der Zeijst, and S. G. Siddell.** 1983. Coronavirus mRNA synthesis involves fusion of non-contiguous sequences. EMBO J. **2**:1839–1844.
30. **Spaan, W. J. M., P. J. M. Rottier, M. C. Horzinek, and B. A. M. van der Zeijst.** 1981. Isolation and identification of virus-specific mRNAs in cells infected with mouse hepatitis virus (MHV-A59). Virology **108**:424–434.
31. **Staden, R.** 1986. The current status and portability of our sequence handling software. Nucleic Acids Res. **14**:217–233.
32. **Stohlman, S. A., R. S. Baric, G. N. Nelson, L. H. Soe, L. M. Welter, and R. J. Deans.** 1988. Specific interaction between coronavirus leader RNA and nucleocapsid protein. J. Virol. **62**:4288–4295.
33. **Tabor, S., and C. C. Richardson.** 1987. DNA sequence analysis with a modified bacteriophage T7 DNA polymerase. Proc. Natl. Acad. Sci. USA **84**:4767–4771.
34. **Weiss, B., H. Nitschko, I. Ghattas, R. Wright, and S. Schlesinger.** 1989. Evidence for specificity in the encapsidation of Sindbis virus RNAs. J. Virol. **63**:5310–5318.